



Conformational studies on resiniferatoxin (RTX), an ultrapotent vanilloid agonist

Sam F. Victory^a, Giovanni Appendino^{b†}, David G. Vander Velde^{a*‡}

^aDepartment of Medicinal Chemistry, University of Kansas, Lawrence, KS 66045, U.S.A.

^bDipartimento di Scienza e Tecnologia del Farmaco, via Giuria 9, 10125 Torino, Italy

Received 24 June 1997; accepted 30 September 1997

Abstract

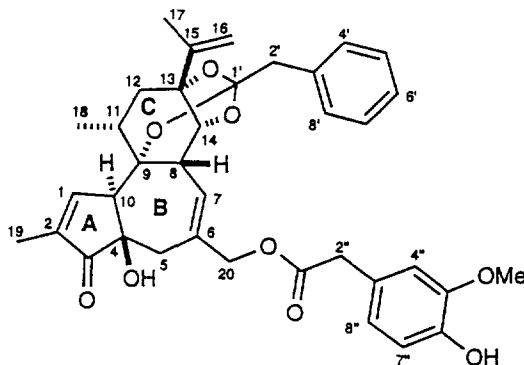
In polar solution, NOE studies show a pronounced clustering of the aromatic moieties (9,13,14-phenylacetate ortho-ester and 20-homovanillate) of the ultrapotent vanilloid agonist resiniferatoxin (RTX). This clustering is absent in nonpolar solution. Low energy clustered structures from molecular dynamics simulations account for the observed NOEs. These results suggest that the phenylorthoacetate moiety can assist the attainment of specific alignments between the terpenoid core and the vanillyl moiety, possibly preorganizing them for ideal receptor binding. © 1998 Elsevier Science Ltd. All rights reserved.

Keywords: Resiniferatoxin, conformation, NMR, hydrophobic collapse.

1. Introduction

Resiniferatoxin (RTX) is a daphnane diterpenoid contained in the irritant latex of some succulent African Euphorbias (*E. resinifera* Berg, *E. posonii* Pax., *E. unispina*) [1,2]. RTX was isolated because of its extraordinary potency in the mouse-ear erythema assay, where it outperforms the activity of tetradecanoyl-phorbol acetate (TPA) by a factor of a thousand [1c]. RTX and phorbol esters, though structurally and biogenetically related, have different cellular endpoints, since RTX failed to bind the protein kinase C isoforms targeted by phorbol esters and did not behave as a tumor promoter [1c]. Interest in RTX was rekindled by the discovery that it acts as an ultrapotent analog of capsaicin, the pungent constituent of hot peppers [3]. Specific binding of [³H]RTX provided the first direct proof for the existence of a recognition site in dorsal root ganglia for a class of pungent natural products encompassing, besides capsaicin [4], polygodial type sesquiterpene dialdehydes [5] and certain prenylated aromatics [2]. This site has

been traditionally referred to as the ‘vanilloid receptor’, though some of the recently discovered ligands actually lack the vanillyl moiety [1,5]. None of these biological analogues approach the potency of RTX, whose therapeutic potential is also wider [6]. Indeed, animal experiments have shown that RTX is able to fully desensitize against chemogenic pain without any apparent toxicity [6], and the compound is undergoing clinical trials for the treatment of diabetic neuropathy [2].



Resiniferatoxin (RTX)

*Corresponding author.

†e-mail: appendino@ch.unito.it

‡e-mail: svictory@ukans.edu; dvandervelde@ukans.edu

The pharmacophore of RTX is still ill defined. Structure-activity studies on the natural product have highlighted the relevance of the orthoester group on ring C, the keto group on ring A, and the vanillyl moiety for significant activity [7,8]. The synthesis of a series of phorbol-RTX hybrids further highlighted the role of the functionalization around ring C for vanilloid activity, since changes in binding mode and affinity were observed in chimeric compounds combining the functionalization pattern of RTX in rings A and B and that of phorbol esters in ring C [9]. The phenylorthoacetate group of RTX can in theory act as a conformational lock for ring C, locking it in a boat conformation,

and/or help the attainment of specific alignment(s) between the homovanillyl moiety and the terpenoid core through noncovalent hydrophobic interactions. An ideal alignment between the moieties is presumably responsible for the ultrapotency of RTX compared with flexible (capsaicin) or simpler analogues (sesquiterpene dialdehydes), but no information on the bioactive conformation(s) of any of these compounds is available. The location of the binding site on the receptor protein and its surrounding environment are also unknown.

Rich and coworkers [10] have suggested that for molecules whose conformation depends on the medium, the conformation(s) populated in polar media are the

Table 1
Chemical shift and NOEs for RTX in 75% DMSO-*d*₆/25% D₂O

Number	¹³ C shift	¹ H shift	¹ H shift ^a	NOE ^b
1	158.4	7.44	7.44	18, 19, 4' s; 10, 11, 17 m; 8, 14, 2', 4'', 7'', OCH ₃ w
2	137.6	—	—	
3	209.5	—	—	
4	73.5	—	—	
5a	39.2	2.40	2.43	
5b		1.88	2.05	18 m
6	135.7	—	—	
7	128.6	5.79	5.88	
8	39.2	3.05	3.08	17, 18 s; 10, 11, 12b m; 14, 2' w
9	82.3	—	—	
10	55.7	2.78	3.05	5b, 12a, 18 s; 11, 19 m; 17 w
11	33.5	2.51	2.55	18 s; 12a, 12b, 17, 19 m
12a	36.2	2.11	2.11	12b, 17, 18 s
12b		1.41	1.55	18 s
13	85.1	—	—	
14	80.8	4.27	4.20	19 m; 18 w
15	146.9	—	—	
16	111.7	4.71	4.70	
17	19.5	1.52	1.52	18 s; 12b m
18	20.8	0.93	0.96	
19	11.0	1.75	1.82	18 s; 17 w
20	70.7	4.56	4.57	
1'	118.3	—	—	
2'	41.5	3.15	3.21	17, 19 w
3'	126.3	—	—	
4', 8'	131.6	7.34	7.37	2', 6' s; 16, 17, OCH ₃ m; 7, 8, 10, 14, 18, 2'', 8'' w
5', 7'	128.8	7.32	7.29	
6'	127.6	7.28	7.24	
1''	173.0	—	—	
2''	41.4	3.57	3.56	7, 10, 4' w
3''	— ^c	—	—	
4''	113.9	6.82	6.80	2'', 7'', 8'', OCH ₃ s; 5b, 7, 10 w
5''	148.3	—	—	
6''	145.8	—	—	
7''	116.0	6.75	6.84	2'' s; 10, 11 m; 7, 14, 17, 19, OCH ₃ w
8''	122.5	6.71	6.76	
MeO	56.5	3.73	3.88	2'' s; 19 m; 17, 18, 2' w

^aIn CDCl₃.

^bs = strong; m = medium; w = weak.

^cObscured by overlap.

most likely to be recognized by a receptor and to resemble the bound conformation, cyclosporin A being a prominent example. Polar solvents will favor conformers where hydrophobic groups cluster together ('hydrophobic collapse'). We have now carried out an NMR investigation on RTX in both polar and nonpolar solutions, and determined that its preferred conformations are solvent dependent. Evidence for clustering of the two aromatic moieties attached to the rigid daphnane core was found in polar solution, and molecular dynamics simulations were used to identify low-energy structures which were consistent with the NMR data.

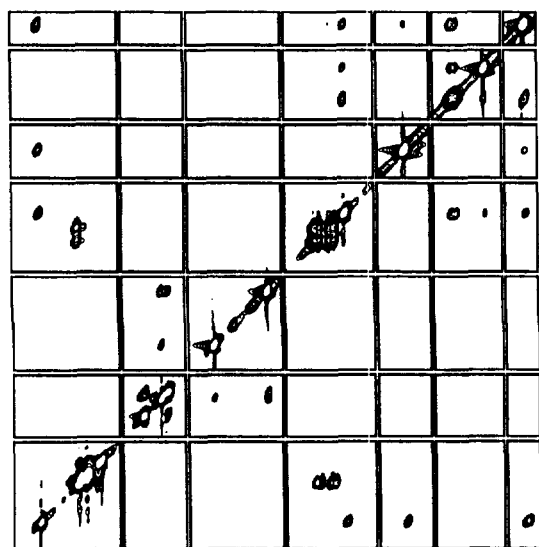
2. Results and discussion

2.1 Nuclear magnetic resonance studies

Proton and carbon assignments for RTX were confirmed using a combination of 1-D and 2-D techniques. These are shown in Table 1; a limited number of ^1H shifts [1] and complete ^{13}C shifts [11] (both in CDCl_3) have previously been published.

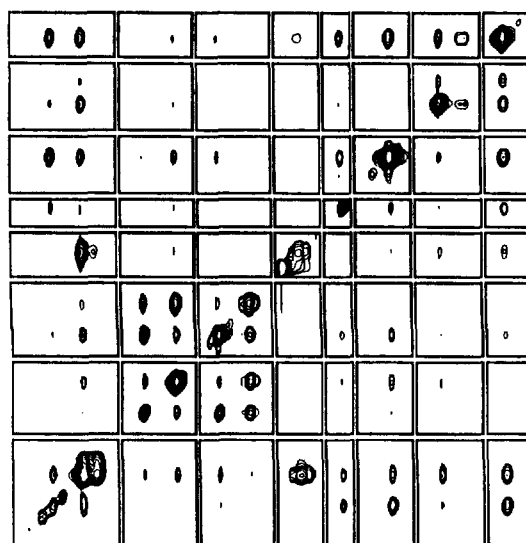
NOE connectivities were identified in both solvents at room temperature (ROESY) and at subambient temperature (NOESY), where the correlation time of the molecule is sufficiently long that all NOEs are negative. NOESY has the advantages over ROESY that the mixing time can be made as long as desired without

consideration of how the probe hardware will react to the spinlock, and there are fewer artifacts. In our hands, spectra of flexible molecules taken under these conditions have been more informative than those taken at room temperature [12]. The temperatures were chosen to be as low as possible prior to the onset of line broadening due to freezing or high viscosity (-10°C in $\text{DMSO}/\text{D}_2\text{O}$, -60°C in CDCl_3), and the proton T_1 s were measured. For the NOESY spectra, the mixing time was set to 500 ms in CDCl_3 and 1 s in $\text{DMSO}/\text{D}_2\text{O}$, or approximately 75% of the average T_1 of the aromatic protons to yield optimal intensities for these slow-relaxing signals. Although the same crosspeaks are observed in both ROESY and NOESY, and there were no sizable changes in chemical shifts, from which it appears that the same conformations are populated at both ambient and sub-ambient temperatures, weak signals were much less likely to be obscured by vertical streaks in the NOESY, so these are the spectra shown (Figs 1 and 2). 47 NOEs were observed in CDCl_3 ; all but two were internal to the ester groups or to the daphnane core of the molecule, which has very limited conformational flexibility; consequently these NOEs provide little conformational information. (The two ester-core NOEs observed were between H-16 in the daphnane core and the 4'-8' protons on the phenylorthoacetate ester, and H-7 in the daphnane core and 2'' on the C-20-homovanillate ester; these are also not indicative of a preferred conformation.) In nonpolar solvent, the ester



1, 4'-8' 7'', 4'', 8'', 7''OCH₃, 2'' 2', 10 19 17, 12b 18

Fig. 1. Tile plot of RTX NOESY spectrum in CDCl_3 , -60°C , 500 ms mixing time, showing aromatic signals from the esters and selected regions of the daphnane core.



1, 4'-8' 4'', 8'', 7''OCH₃, 2'' 2', 10 19 17, 12b 18

Fig. 2. Tile plot of RTX NOESY spectrum in $\text{DMSO}/\text{D}_2\text{O}$, -10°C , 1 s mixing time, showing the same peaks illustrated in Fig. 1.

groups are likely extended away from the center of the molecule and from each other, based on the minimal number of NOEs between these groups. However, in DMSO–D₂O, a total of 77 NOEs were observed; 28 of these connected the homovanillate ester and phenylorthoacetate ester groups with each other and with the diterpene core (listed in Table 1). For proper interpretation of these new NOEs, it is essential to know whether they are intramolecular or intermolecular in origin (the latter would be possible if RTX were aggregating under these conditions.) Although no line broadening suggestive of aggregation was observed in the spectrum, in order to rule this possibility out, the hydrodynamic radius of RTX in DMSO/D₂O was determined as follows. The diffusion coefficient (*D*) of RTX was measured to be $1.24 \times 10^{-6} \text{ cm}^2/\text{s}$ at 25°C, and the viscosity of the solvent mixture (η) was measured as 3.158 cSt. From these values a hydrodynamic radius (*r*) of 5.6 Å was calculated from the Stokes–Einstein equation, $D = kT/6\pi\eta r$, which from inspection of the low energy conformers (see below), is fully consistent with RTX being completely monomeric in solution. Consequently, the core/ester and ester/ester NOEs appear to be intramolecular in origin, and they indicate a propensity for the pendant ester groups to cluster together in polar solution, and also indicate there are preferred orientations of the esters with respect to the core. The dramatic differences observed in the NOESY spectra are illustrated in the tile plots in Figs 1 and 2. In DMSO/D₂O, the phenylorthoacetate ring shows NOEs to H-1, 7, 10, 14, 16, 17, 18, and 19. The 20-homovanillate shows NOEs to the allylic methyl H-19, the allylic methine H-10 and the H-17 methyl. Between the ester groups, there are aromatic-aromatic NOEs, NOEs from the methylene protons linking each ring to the core (2', 2'') to the aromatic protons on the other ring, and NOEs from the methoxy group on the 20-ester to the orthoester. (These extra crosspeaks do not appear in the CDCl₃ NOESY displayed at any level above the noise.)

2.2 Molecular modeling studies

Application of the NOE-derived NMR distance constraints in DMSO/D₂O for the pendant ester groups in an initial energy minimization produced considerable structural distortion, clearly showing that the constraints could not all be satisfied in a single reasonable structure. This is as expected since the vanillyl moiety is freely rotatable, and the orthoester possesses mobility in its benzyl moiety. Consequently, we chose to perform unrestrained molecular dynamics simulations, identify families of low-energy structures, and then to compare these structures to the NMR data. This process yielded five structures whose variability was essentially all in the ester groups. The orthoester, whose conformational flexibility is more limited, will be described first. Four of

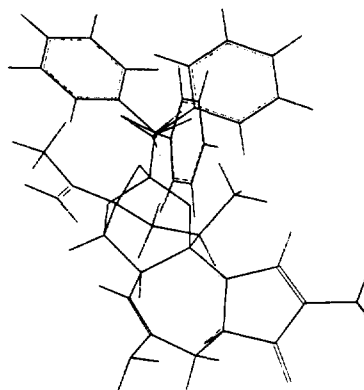


Fig. 3. View of RTX showing three low-energy orientations of the orthoester group. For clarity, the homovanillyl group is not shown.

the structures show the orthoester in essentially the same orientation, tucked close to the daphnane core, with the torsion angle O9–C1'–C2'–C3' with a value within a few degrees of 60°. In the fifth structure, this group is rotated –110°, and the orthoester benzyl ring appears to be pi-stacked with the homovanillyl ring. However, this structure was present only for a relatively short time at the beginning of the dynamics simulation, and was not observed to reappear. The third plausible rotamer of this group would be staggered approximately 120° from the other two, although this orientation did not appear among the low-energy structures resulting from our dynamics simulation. Manual adjustment of the torsion angle in the model, followed by energy minimization, gave a value of 170°. (In Ref. 8, the orthoester is apparently shown in this position, which extends it relatively far away from the daphnane core, in particular from the A ring.) These three orientations are illustrated in Fig. 3. Distances from the *ortho* (4') protons (which appeared to be closer than the *meta* in all cases, though in the NOESY the two signals could not be completely separated), to the protons in the diterpene core with which NOEs were observed, are shown in Table 2. From the table and the figure, it is evident that the only NOEs that would be observed from the 170° rotamer would be to H-16 or 17 (depending on rotation around the C13–C15 bond). In CDCl₃, the NOE to

Table 2
Interproton distances (Å) involving orthoester ring (minimum distances from *ortho* protons)

Torsion	1	7	10	14	16 ^a	17 ^a	18	19
–50°	2.8	3.0	2.8	4.3	5.5	5.0	5.0	>6
60°	2.8	5.3	3.7	>6	3.9	3.3	3.2	5.0
170°	>6	4.7	>6	4.7	3.2	3.5	3.7	>6

^aThese distances were measured with rotation around the freely rotatable C13–C15 bond to determine the minimum distance.

H-16 is the only one observed. NOEs to both are observed in DMSO/D₂O, along with the others tabulated, indicating appreciable population of the other rotamer(s) where the aromatic ring lies closer to the core. Most of the NOEs observed in DMSO/D₂O between the orthoester and the daphnane can be accommodated by the 60° rotamer, with the exception of those to H-7 and 14, for which the only satisfactory contacts are found in the –50° rotamer. Our inter-

pretation is that the occupancy of the orientations of the orthoester in polar solvent is 60° > –50° > 170°.

Turning now to the C-20 homovanillyl ester, in the models it is observed to occupy three clustered and two extended orientations (see Fig. 4). In the first structure (A), the vanillyl moiety lies relatively close to the A ring, consistent with the observed NOE to H-1 (aromatic protons within 2.7 and 3.3 Å), and close enough to the orthoester ring to produce aromatic-aromatic NOEs

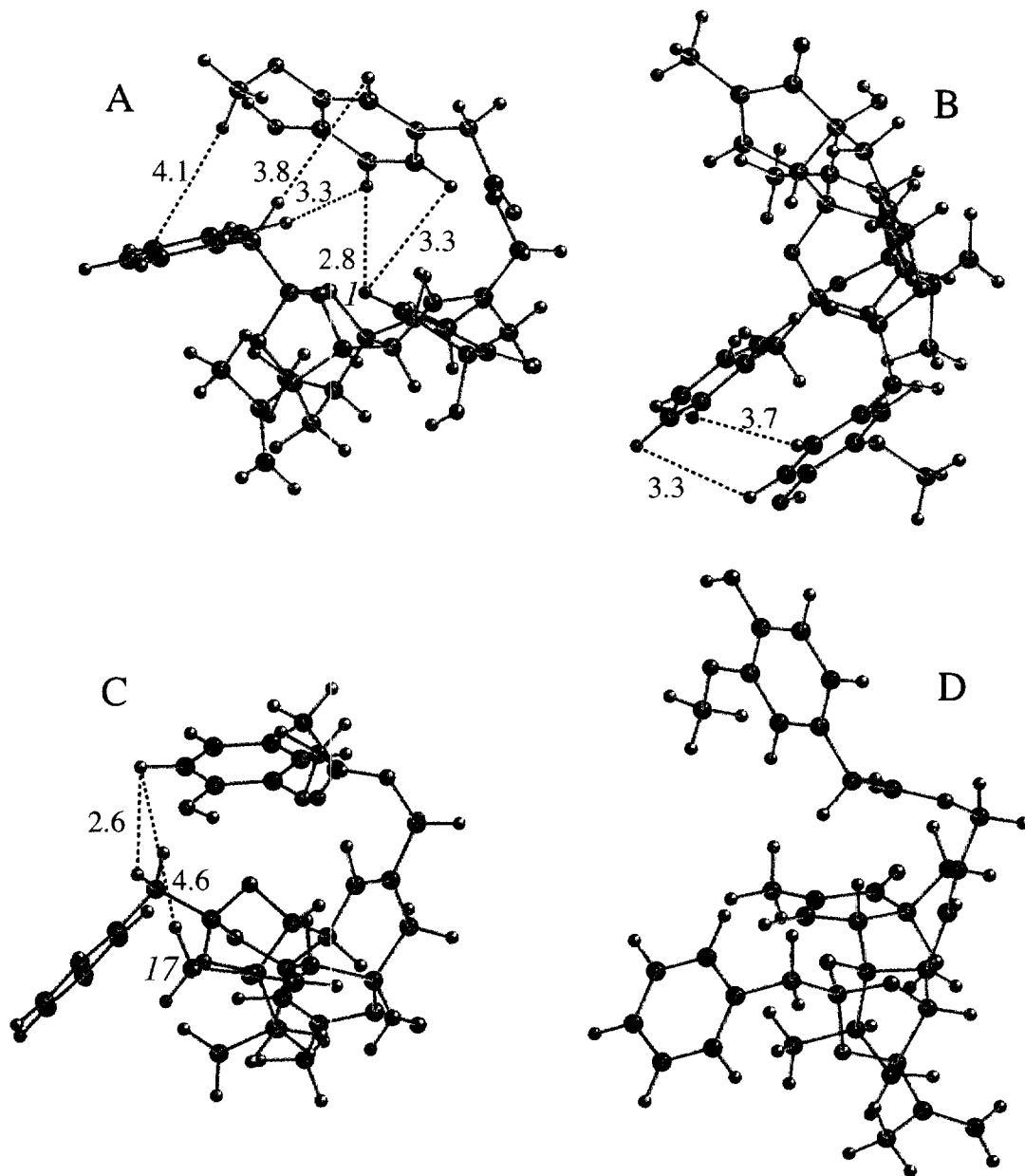


Fig. 4. Ball and stick representations of four of the five unique conformations of RTX from molecular dynamics simulations. Dotted lines indicate NOEs observed between the homovanillyl group and the rest of the molecule; the distances between the protons in each of the conformers are shown in Roman type, atom numbers in *italic*.

(as close as 3.3 Å). In two of the structures (B and C), it lies close enough to the 17 methyl to produce the NOEs observed to the homovanillyl group (Me-OMe protons within 2.7 Å; aromatics within 4 Å). The two aromatic rings are stacked in structure B, again close enough to contribute to the observed aromatic-aromatic NOEs (also within 3.3 Å). In the third structure, aromatic protons from the homovanillyl group approach the 2' protons. In structure D, the C-20 ester is extended well away from the rest of the molecule. The fifth structure (not shown) is essentially identical to D except for a 180° rotation of the 2''–3'' bond, with the aromatic ring still extended away from the rest of the molecule.

In CDCl₃, the extended conformation(s) seem to be dominant for the homovanillate as well as the orthoester group, based on the absence of any detectable long-range NOEs. In DMSO/D₂O, there must be rapid averaging between structures similar to A–C shown here, because, for example, the homovanillate group cannot simultaneously be close to H-1 and H-17, though both NOEs are present. (The simultaneous appearance of these and several other NOEs to two well separated areas of the core is the reason why no single structure can simultaneously satisfy all the NOE constraints). Although more than a single conformation must exist in polar solution, it is clear that the phenylorthoester can not only act as a conformational lock for ring C, but also assist the attainment of specific alignments between the terpenoid core and the vanillyl moiety. Similar clustering effects are also possible for the 2'-nor analogue of RTX, an active analogue where the phenylorthoacetate moiety is replaced by an orthobenzoate moiety [8].

From the models, end-to-end distances (approximate molecular diameters) of 10–12 Å were measured in Sybyl for the three 'collapsed' conformers. The extended conformers had approximate diameters along their longest axes in excess of 15 Å. The experimentally measured hydrodynamic radius of 5.6 Å in DMSO/D₂O is therefore strong evidence that RTX is both overwhelmingly monomeric and adopting compact conformations in this solvent mixture.

3. Conclusion

RTX consists a relatively rigid terpenoid core, to which two flexible aromatic appendices are bound. The vanillyl moiety is necessary for binding, and the phenylorthoacetate for ultrapotency [8,9]. In nonpolar solution, the aromatic groups are found extended away from the core, the orthoester in the ~170° rotamer, with only two NOEs required by covalent geometry being detected between the core and the esters. This is in agreement with a previously published low energy structure of RTX [8]. In polar solution, however, the

aromatic moieties show a pronounced clustering, evidenced by the detection of numerous NOE correlations. Both of the ester groups adopt different orientations in order to make this clustering possible.

4. Experimental

RTX was purchased from LC Labs (Woburn, MA) and used without further purification. 5 mg of compound was dissolved in 0.5 ml CDCl₃ or 75% DMSO/*d*₆/25% D₂O. There were no visible impurities in the proton NMR spectrum of a freshly prepared sample, so the purity of the sample can be estimated as >98%. NMR data was acquired on a Bruker AM-500 (NOESY, diffusion measurements) and Avance DRX-400 (ROESY, HMQC, COSY), using standard Bruker hardware and pulse programs except for the diffusion measurements. These were performed with an auxiliary PC-driven 15 ampere gradient pulse generator (Digital Specialties, Chapel Hill, NC) interfaced to the Bruker Aspect 3000 computer, and a Bruker 5 mm inverse broadband probe with a z-axis gradient coil. The data was acquired using the pulsed field gradient bipolar longitudinal eddy current delay pulse sequence [13]. The diffusion delay time was fixed at 200 ms and the gradient pulse duration at 1 ms. Twenty spectra were acquired with the gradient pulse amplitude incremented from 0.5 to 6.9 amperes. The experimental gradient strength was calculated from a coil constant of 5.15 G/cm/A based on the known diffusion coefficient of water at room temperature, $2.36 \times 10^{-5} \text{ cm}^2/\text{s}$. The diffusion coefficient of RTX was obtained from the slope a semilog plot of peak height versus the square of the gradient strength.

The NMR data was processed and analyzed on a Silicon Graphics Indigo 2 running Felix 95 (Molecular Simulations Inc.). Molecular dynamics and energy minimization were performed on an SGI Indigo 2 running Sybyl 6.2 (Tripos). Prior to dynamics, partial atomic charges were calculated using the Gasteiger-Hückel method as implemented in Sybyl, and the structure was minimized using the standard Tripos force field. A 100 ps molecular dynamics simulation was performed in vacuo at 400K with a time step each 1 fs with a structure saved each 50 fs (generating 2000 conformers). The above-ambient temperature was chosen to speed the computations by sampling a wider variety of conformations during a simulation of reasonable length. Both the simulation and the experimental data suggest that the interconversions between the low energy conformations are rapid.

The structures were then minimized with the SPL Sysmin macro of Sybyl, and structures with an RMS deviation >0.125 from any previously saved structure were retained. This resulted in approximately 120 structures, but from visual inspection, it was evident that

many were very similar. The Sysmin procedure was repeated with the deviation threshold increased to 0.175, and the number of unique structures was reduced in this case to five. Viscosity measurements were performed with a Cannon-Ubbelohde type 75 semi-micro viscometer (Cannon Instrument Co., State College, PA) suspended in a water bath at 25°C.

Acknowledgements

The authors thank the Kansas Health Foundation for a postdoctoral fellowship awarded to SFV; and Arpad Szallasi, Department of Anatomy and Neurobiology, Washington University School of Medicine, St Louis, MO, Peter Blumberg, National Cancer Institute, Bethesda, MD, and Cynthia Larive, University of Kansas, for helpful discussions.

References

- [1] (a) Hergenbahn M, Adolf W, Hecker E. *Tetrahedron Lett* 1975;1595. (b) Evans FJ, Schmidt RJ. *Phytochemistry* 1976;5:333. (c) Revised structure: Adolf W, Sorg B, Hergenbahn M, Hecker E. *J Nat Prod* 1982;45:347.
- [2] For a recent review on the history and pharmacology of RTX, see: Appendino G, Szallasi A. *Life Sci* 1997;60:681.
- [3] Szallasi A, Blumberg PM. *Neuroscience* 1989;30:515.
- [4] Szallasi A. *Gen Pharmacol* 1994;25:223.
- [5] Szallasi A, Jonassohn M, Acs G, Biro T, Acs P, Blumberg PM, Sterner O. *Br J Pharmacol* 1996;119:283.
- [6] Szallasi A, Blumberg PM. *Adv Pharmacol* 1993;24:123.
- [7] Szallasi A, Sharkey NA, Blumberg PM. *Phytother Res* 1989;3:253.
- [8] Walpole CSJ, Bevan S, Bloomfield G, Breckenridge R, James IF, Ritchie T, Szallasi A, Winter J, Wrigglesworth R. *J Med Chem* 1996;39:2939.
- [9] Appendino G, Cravotto G, Palmisano G, Annunziata R, Szallasi A. *J Med Chem* 1996;39:3123.
- [10] (a) Wiley RA, Rich DH. *Med Res Rev* 1993;3:327. (b) Rich DH. In Testa B, Kyburz E, Fuhrer W, Giger W, editors. *Perspectives in Medicinal Chemistry*. VCH: New York, 1993:15–25.
- [11] Fatope MO, Zeng L, Ohayaga JE, Shi G, McLaughlin JL. *J Med Chem* 1996;39:1005.
- [12] (a) Vander Velde DG, Georg GI, Grunewald GL, Gunn CW, Mitscher LA. *J Am Chem Soc* 1993;115:11650. (b) Victory SF, Vander Velde DG, Jalluri RK, Grunewald GL, Georg GI. *Bioorg Med Chem Lett* 1996;6:893.
- [13] Wu D, Chen A, Johnson CS Jr. *J Magn Reson* 1995;115:260.